RSC Advances

ROYAL SOCIETY OF CHEMISTRY

www.rsc.org/advances

Copper (II) phthalocyanine supported on three-dimensional nitrogen-doped graphene/PEDOT-PSS nanocomposite as highly selective and sensitive sensor for ammonia detection at room temperature

Hamed Sharifi Dehsari[†a], Jaber Nasrollah Gavgani[†a], Amirhossein Hasani[c], Mojtaba Mahyari[*b], Elham Khodabakhshi Shalamzari[a], Alireza Salehi[c], Farmarz Afshar Taromi[*a]

a) Department of Polymer Engineering and Color Technology, Amirkabir University of Technology, P.O.Box 15875-4413, Tehran, Iran
b) Department of Chemistry, Shahid Beheshti University, G. C., P.O.Box 19396-4716, Tehran, Iran
c) Department of Electrical Engineering, K.N. Toosi University of Technology, P.O.Box 16315- 1355, Tehran, Iran

Abstract

Here we present a highly efficient ammonia (NH_3) gas sensor made of copper (II) tetrasulfophthalocyanine supported on three-dimensional nitrogen-doped graphenebased frameworks (CuTSPc@3D-(N)GFs)/ poly(3,4-ethylenedioxythiophene)-poly(styrenesulfonate) (PEDOT-PSS) nanocomposite sensing film with high uniformity over a large surface area. The NH_3 gas sensing performance of the nanocomposite was also compared with those of the sensors based on pure PEDOT-PSS and pristine CuTSPc@3D-(N)GFs. It was revealed that the synergetic behavior between both of the candidates allowed excellent sensitivity and selectivity to NH_3 gas in a low concentration range of 1–1000 ppm at room temperature. The CuTSPc@3D-(N)GFs/PEDOT-PSS

*Email address: afshar@aut.ac.ir; m_mahyari@sbu.ac.ir
Tel: +982164542401
[†]First two authors contributed equally to this work.

nanocomposite gas sensor exhibited much better (~ 5 and 53 times, respectively, with the concentration of NH_3 gas at 200 ppm) response to NH_3 gas than those of the pure PEDOT-PSS and pristine CuTSPc@3D-(N)GFs gas sensors. The combination of the CuTSPc@3D-(N)GFs and PEDOT-PSS facilitated the enhancement of the sensing properties of the final nanocomposite, and pave a new avenue for the application of CuTSPc@3D-(N)GFs/PEDOT-PSS nanocomposite in the gas sensing field.

Keywords: CuTSPc@3D-(N)GFs/PEDOT-PSS nanocomposite, Gas sensor, NH_3 detection, Conducting polymer

Introduction

Graphene, as a two-dimensional of sp^2 bonded carbon sheet, has attracted much attention in many divers application especially chemical sensors [1-8] owing to its excellent electronic, high mechanical stiffness and specific surface-to-volume ratio, as well as superior conductivity [9-12]. Three-dimensional (3D) graphene-based frameworks (3D-GFs) such as sponges, foams, and aerogels are an important class of new-generation porous carbon materials, which exhibit high porosity, large surface area, and high electrical conductivity [13-17]. These materials can serve as strong matrix for functionalizing metal, metal oxide, and electrochemically active polymers for various applications in electrochemical capacitors [18-20], batteries [21, 22], catalysis [23-25]. In the following, Dong et al. [26] demonstrated that 3D graphene electrode as an electrochemical sensor for detection of dopamine exhibited remarkable sensitivity (619.6 μA mM^{-1} cm^{-2}) and lower detection limit (25 nM at a signal-to-noise ratio of 5.6), with linear response up to ~ 25 μM. Therefore, 3D-GFs can provide a promising platform for the development of high performance electrochemical sensors for dangerous volatile organic compounds (VOCs).

Poly(3,4-ethylenedioxythiophene)-poly(styrenesulfonate) (PEDOT-PSS) as conjugated polymer (a mixture of two ionomers) has been extensively studied as the active material in sensing applications because of its good electrical conductivity, high transparency, low redox potential and good processability [27-29]. Nevertheless, its limited chemical and structural properties prevent its use in various practical applications especially electrochemical sensing [30]. It seems that the PEDOT-PSS composites with carbon nanostructures could be promising solution to its failures. In the following, Jian et al [31] used PEDOT-PSS composite film with O_2 plasma-treated single-walled carbon nanotubes for detection of ammonia (NH_3) and trimethylamine gases. Seekaew et al [27] reported the NH_3 sensing behavior of graphene-PEDOT-PSS composite film at room temperature. These evidence indicate that PEDOT-PSS composite films show potential as useful sensing materials, but their low sensivity restrict their application in practical VOC sensors.

Because the above-mentioned reasons and also our interest in the synthesis of graphene based materials for various applications [25, 32-34], especially as new sensors [35-37], herein, we demonstrate the use of copper (II) tetrasulfophthalocyanine supported on three-dimensional

nitrogen-doped graphene-based frameworks (CuTSPc@3D-(N)GFs) and PEDOT-PSS nanocomposite as a novel gas sensor. This new architecture holds great appeal as a chemical sensor owning to large surface area, 3D multiplexed and highly conductive pathways, and continuously interconnected macroporous structures as well as modified active surface. To demonstrate its potential, we used it here for the detection of NH_3 as highly toxic gas which leads to irritates skin, eyes and respiratory tract of humans.

Experimental

Preparation of CuTSPc@3D-(N)GFs/PEDOT-PSS nanocomposite

The CuTSPc@3D-(N)GFs were synthesized based on our previous work [25]. The obtained CuTSPc@3D-(N)GFs were dispersed in DI water (~ 1 mg/ml) and mildly sonicated for 30 min in a bath sonicator (EUROSONIC® 4D, 50 kHz). The PEDOT-PSS aqueous solution (weight ratio = 1-6, Clevios™ P VP AI 4083, solid content 1.3–1.7 %) was first dissolved in a DI water with a weight concentration of 89.82 %. The CuTSPc@3D-(N)GFs dispersion with 6 wt% Dimethyl sulfoxide (DMOS, Sigma-Aldrich Co) were added into the PEDOT-PSS solution and a homogeneous aqueous dispersion was obtained after 2 h stirring and sonicated for 30 min.

Fabrication of CuTSPc@3D-(N)GFs/PEDOT-PSS nanocomposite gas sensor

The nanocomposite gas sensor was prepared from PEDOT-PSS and CuTSPc@3D-(N)GFs materials with chemical structures schematically illustrated in Fig. 1. For fabrication of CuTSPc@3D-(N)GFs/PEDOT-PSS nanocomposite gas sensor, interdigitated Au electrodes with 100 nm thickness were deposited on a SiO_2/Si substrate (10×4 mm^2) by physical vapor deposition method. The prepared CuTSPc@3D-(N)GFs/PEDOT-PSS nanocomposite solution was then drop casted over an interdigitated electrode (Fig. 2a). The width and inter-spacing of the electrodes are 200 µm and 400 µm, respectively. Then the nanocomposite gas sensor was backed for 1 h in furnace (Exciton, EX1200-4L) at 80 °C in nitrogen atmosphere (Fig. 2b). The pristine CuTSPc@3D-(N)GFs and PEDOT-PSS gas sensors were also fabricated and tested for comparison. The fabricated CuTSPc@3D-(N)GFs/PEDOT-PSS nanocomposite gas sensor is displayed in Fig. 2c,d.

Characterization methods

Transmission electron microscopy (TEM) was examined under LEO 912AB electron microscopy operated at an accelerating voltage of 120 kV. Scanning electron microscopy (SEM) was measured with S-4160 electron microscopy. Atomic force microscopic (AFM) images were

performed in the tapping mode with an ARA AFM (0201/A, Ara research Co, Iran). Brunauer–Emmett–Teller (BET) surface area measurements were carried out by nitrogen adsorption at 77 K using an ASAP2020 instrument. The conductivity of sensing films was measured by 4-point technique probe at 10 nA applied current. The sensor resistances were measured in a closed steel chamber (lab-made) with a LCR meter (Pintek-LCR900) and vapor gas flows were injected into the closed steel chamber by a mass flow meter (Alicat scientific, Tucson, USA). The reference humidity and sensor temperature were monitored by PT100 and HIH4000, respectively. The response and selectivity of the gas sensors were then assessed by the standard flow-through method towards NH_3, methanol, ethanol, acetone, toluene, chlorobenzene, and water with gas concentrations ranging from 1 ppm to 1000 ppm at room temperature. A constant flux of synthetic air of about 50 $cm^3.min^{-1}$ was mixed with the NH_3 gas source at different flow rate ratios to desired concentrations using mass flow controllers. All experiments were performed at room temperature (25 ± 2 °C) and the relative humidity of 10 ± 2 %. The sensitivity defined by the following equation:

$$\text{Sensitivity}=\frac{\Delta R}{R_0}\times 100 \qquad (1)$$

and

$$\Delta R = R_{gas} - R_0 \qquad (2)$$

where R_0 and R_{gas} are the resistances of the sensor in synthetic air and test gas, respectively.

Results and discussion

The surface morphology of the CuTSPc@3D-(N)GFs has been presented in the SEM and TEM images of Fig. 3a-b, respectively. Fig. 3a exhibits the 3D morphology and an interconnected porous structure ultrathin graphene nanosheets. Moreover, the pore size ranges from a few hundred nanometers to several micrometers. Fig. 3b not only clearly shows the presence of mesopores in the carbon walls, but also reveals a wrinkled paper-like texture to the sheets, consistent with previous reports [38]. In addition, based on the BET method, the synthesized support (3D-(N)GFs) in our previous work has a high surface area (up to 266.0 $m^2.g^{-1}$) to put CuTSPc as active sensing sites. The chemical composition of 3D-(N)GFs and CuTSPc@3D-(N)GFs was confirmed by several characterization method such as elemental analysis, fourier

transform infrared spectroscopy, thermogravimetric analysis, X-ray powder diffraction and X-ray photoelectron spectroscopy [25].

Fig. 4a-b show the surface morphology of drop-coated pure PEDOT-PSS and CuTSPc@3D-(N)GFs/PEDOT-PSS nanocomposite film, respectively. As can be seen that the pure PEDOT-PSS has relative smooth surface (Fig. 4a). On the other hand, Fig. 4b exhibits that the CuTSPc@3D-(N)GFs are uniformly dispersed into the PEDOT-PSS matrix without obvious agglomeration. This was ascribed to the hydrophilic nature of CuTSPc on the surface of the 3D-(N)GFs which not only ensured the strong bonding with PEDOT-PSS but also improved the dispersity and stability of the CuTSPc@3D-(N)GFs in aqueous solution (Fig. S1). Further roughness evaluations by AFM show that the average surface roughness (R_a) of pure PEDOT-PSS films is 1.98 nm while R_a of the CuTSPc@3D-(N)GFs/PEDOT-PSS is 7.52 nm (Fig. S2). The much larger R_a of CuTSPc@3D-(N)GFs/PEDOT-PSS nanocomposite film compared to its PEDOT-PSS film suggests a significant enhancement of the active surface-area for gas adsorption by CuTSPc@3D-(N)GFs [25, 27].

Fig. 5a shows dynamic response of the CuTSPc@3D-(N)GFs/PEDOT-PSS nanocomposite gas sensor towards 1000 ppm NH_3 at room temperature in air. It exhibits that the sensor presents good repeatability of response towards repeated NH_3-sensing cycles at room temperature. The sensivity of the nanocomposite gas sensor increases upon exposure to NH_3 and recovers to the initial value upon the removal of NH_3 in air. As shown in Fig. 5b, the sensivity of the CuTSPc@3D-(N)GFs/PEDOT-PSS nanocomposite gas sensor increases dramatically when exposed to various concentrations of NH_3 ranging from 200 ppm to 800 ppm, and recovers towards the original values when NH_3 is replaced by air. The changing behavior of sensivity may be ascribed to the adsorption and desorption of NH_3 molecules of the nanocomposite sensing film [27]. The details of sensing mechanism for CuTSPc@3D-(N)GFs/PEDOT:PSS nanocomposite gas sensor will be discussed in further. In addition, the conductivities of pure PEDOT-PSS and CuTSPc@3D-(N)GFs/PEDOT-PSS nanocomposite sensing films are 650 and 1430 Scm^{-1}, respectively. It indicates that the conductivity of pure PEDOT-PSS is increased by more than two factor, leading to significant increase of charge carrier concentration owning to CuTSPc@3D-(N)GFs incorporation. Therefore, CuTSPc@3D-(N)GFs shows a dominant effect in the charge transport through the PEDOT-PSS matrix.

The PEDOT-PSS based gas sensors usually operate at rather low temperatures with respect to gas sensors based on metal oxide [27, 35, 39]. It can be seen that the CuTSPc@3D-(N)GFs/PEDOT-PSS nanocomposite gas sensor shows low sensitivity to NH_3 with increase of temperature (Fig. 6). Therefore, the optimal temperature of the CuTSPc@3D-(N)GFs/PEDOT-PSS nanocomposite gas sensor for NH_3 detection was found to be room temperature. Since the interaction between CuTSPc@3D-(N)GFs/PEDOT-PSS nanocomposite sensing film and volatile organic compounds (VOCs) gas is exothermic, the activation energy of desorption is larger than that of the adsorption NH_3 molecules of nanocomposite sensing film. This revealed that the decrease in sensivity at higher temperatures is resulted from the higher desorption rate of NH_3 gas.

The response time of the pure PEDOT-PSS and CuTSPc@3D-(N)GFs/PEDOT-PSS nanocomposite gas sensors are estimated to be ~ 6 min and ~ 2.5 min, respectively when it was experiencing the 95 % of the resistance change. Moreover, the recovery time of pure PEDOT-PSS and CuTSPc@3D-(N)GFs /PEDOT-PSS nanocomposite gas sensors are ~ 2.5 min and ~ 1 min, respectively. Therefore, CuTSPc@3D-(N)GFs/PEDOT-PSS nanocomposite gas sensor indicates relatively short response and recovery times compared with PEDOT-PSS one (see Fig.7).

Fig. 8 demonstrates the sensivity of pure PEDOT-PSS, pristine CuTSPc@3D-(N)GFs and CuTSPc@3D-(N)GFs/PEDOT-PSS nanocomposite gas sensors as function of NH_3 concentration at room temperature. At 1000 ppm NH_3 concentration, the sensivity of pure PEDOT-PSS, pristine CuTSPc@3D-(N)GFs and CuTSPc@3D-(N)GFs/PEDOT-PSS gas sensors are 14.8 %, 9 %, and 91 %, respectively. At low concentration (50 ppm), the sensivity as for mentioned gas sensors are 4 %, 0.35 %, and 9 %, respectively (inset of Fig. 8). As can be seen that the room temperature sensivity of pure PEDOT-PSS is less high than that of CuTSPc@3D-(N)GFs, but its response is substantially increased after CuTSPc@3D-(N)GFs incorporation. Thus, CuTSPc@3D-(N)GFs improves NH_3 interaction leading the higher charge reduction only when it is included in PEDOT-PSS network. The detection limit of NH_3 for CuTSPc@3D-(N)GFs/PEDOT-PSS nanocomposite gas sensor is thus estimated to be 10 ppm at the room temperature.

Fig. 9 demonstrates the selectivity of the CuTSPc@3D-(N)GFs/PEDOT-PSS nanocomposite gas sensor to various VOCs vapors at concentration of 200 ppm. The sensivity of the CuTSPc@3D-

(N)GFs/PEDOT-PSS nanocomposite gas sensor to NH_3, methanol, ethanol, acetone, toluene, chlorobenzene, and water are 18.7 %, 9.4 %, 5.5 %, 4.5 %, 2.3 %, 2.9 %, and 4.4 %, respectively. The CuTSPc@3D-(N)GFs/PEDOT-PSS nanocomposite gas sensor exhibits a remarkably high response to NH_3 and is almost sensitive to other VOCs vapors. The performance of the as-prepared nanocomposite gas sensor in this work was better than the previous reports in the literatures towards NH_3 detection (Table 1).

Table 1. Sensivity (S), response time (R_1), recovery time (R_2), studied detection range (D_r), materials (M) and measured temperature (T_m) of the various NH_3 gas sensors.

Authors	S (%)	R_1 (s)	R_2 (s)	D_r (ppm)	M	T_m (°C)
Our work	8 (50 ppm), 91 (1000 ppm)	138	63	1-1000	CuTSPc@3D-(N)GFs/PEDOT-PSS	25
Xu et al. [40]	2 (10 ppm), 12 (70 ppm)	10	10	10-70	PEDOT nanowire	25
Kwon et al. [41]	2.1 (5 ppm), 24 (100 ppm)	< 1	30	5-100	PEDOT nanotube	25
Seekaew et al. [27]	0.9 (5 ppm), 7 (1000 ppm)	180	----	5-1000	Graphene/PEDPT-PSS	25
Jian et al. [31]	0.1 (2 ppm), 33 (300 ppm)	12	18	2-300	SWCNTs/PEDOT-PSS	25
Yoo et al. [42]	0.015 (20 ppm), 0.075 (100 ppm)	100	700	0-100	pf-MWCNT/PANI	25
Tai et al. [43]	1.67 (23 ppm), 5.55 (117 ppm)	18	58	23-141	PANI/TiO_2	25
Matsughi et al. [44]	1.16 (500 ppm)	1500	-	-	PANI	30
Kebiche et al. [45]	7.1 (92 ppm)	834	600	92-4628	PANI	25
Hong et al. [46]	0.14 (20 ppm), 0.2 (100 ppm)	14	148	20-2000	Palladium/Polypyrrole	25
Crowley et al. [47]	0.24 (100 ppm)	90	90	1-100	Inkjet-printed PANI	80
Verma et al. [48]	0.9 (200 ppm)	1	420	50-200	PANI	25
Sengupta et al. [49]	2.3 (100 ppm)	120	300	100	PANI	25

PANI: Polyaniline; SWCNTs: Single wall carbon nanotubes; MWCNT: Multi wall carbon nanotube

The improved NH_3 sensing properties of CuTSPc@3D-(N)GFs/PEDOT-PSS nanocomposite gas sensor are mainly ascribed to (i) the increased R_a in CuTSPc@3D-(N)GFs/PEDOT-PSS nanocomposite sensing film compared with PEDOT-PSS one, (ii) inherently sensing properties of CuTSPc@3D-(N)GFs and (iii) π-π interaction by CuTSPc@3D-(N)GFs loading including 3D-(N)GFs as a support and Cu(II) complex as an active site in sensing film. (i) Since, the R_a of sensing film is directly proportional with gas sensivity [27, 50], so the much larger R_a of CuTSPc@3D-(N)GFs/PEDOT-PSS nanocomposite sensing film improves the active surface area

for gas adsorption (ii) It is well-known that graphene under ambient conditions behaves p-type semiconductors like conjugated polymers because their electronic properties can be reversibly controlled by doping/dedoping at room temperature [27, 51-53]. In addition, the electron-withdrawing sulfonic acid groups of the CuTSPc can be viewed as a charge delocalization of holes in the valence band. Therefore, when CuTSPc@3D-(N)GFs gas sensor is exposed to an electron donating gas like NH_3, proton transfer from the sulfonic acid groups of CuTSPc to the nitrogen atoms of NH_3 directly gives the self-doped zwiterionic form. Therefore, depletion of holes from the valence band of CuTSPc@3D-(N)GFs occurs, leading to a significant increase in resistance (iii) NH_3 molecules may interact with not only CuTSPc@3D-(N)GFs and PEDOT-PSS but also π-π bonding between CuTSPc@3D-(N)GFs and PEDOT-PSS [9]. Under the exposure to polar molecules like NH_3, the interaction not only can induce charge-transfer across delocalized π-electrons but also can lead to the formation of neutral polymer backbone and decrease in charge carries resulting in the improved sensing performances.

The NH_3 sensing mechanism of the CuTSPc@3D-(N)GFs/PEDOT-PSS nanocomposite gas sensor may be explained based on three possible mechanisms: (1) According to the reversible reaction [27, 45, 54]: CuTSPc@3D-(N)GFs/PEDOT-PSS$^-$ H^+ + NH_3 $\rightleftarrows$ CuTSPc@3D-(N)GFs/PEDOT-PSS + NH_4^+, the protons transfer from the sulfonic acid groups of CuTSPc to the nitrogen atoms of NH_3 molecules directly gives ammonium ions (NH_4^+). This process is reversible, and in fact, when NH_3 atmosphere is removed, the NH_3 molecules decrease the doping level of CuTSPc@3D-(N)GFs/PEDOT-PSS nanocomposite sensing film by partially compensating for the influence of the initial dopants [55], which may change the resistance. (2) The NH_3 molecules are absorbed on the surfaces of CuTSPc@3D-(N)GFs/PEDOT-PSS nanocomposite sensing film by physisorption, the holes of conductive CuTSPc@3D-(N)GFs/PEDOT-PSS nanocomposite sensing film will interact with the electron-donating NH_3 analyte [27, 54]. The charge transfer from adsorbed NH_3 molecules not only increases the delocalization degree of conjugated π-electrons of nanocomposite sensing film, but also decreases the electrical conductivity of the nanocomposite sensing film [31, 41]. This mechanism is widely adopted for explanation of the change in conductivity of conductive polymer to acidic/basic analytes (doping/dedoping process). (3) The swelling of the CuTSPc@3D-(N)GFs/PEDOT-PSS nanocomposite sensing film can increase the PEDOT distance and decrease the CuTSPc@3D-(N)GF's conductive pathways, leading to significant increase in

resistance of the CuTSPc@3D-(N)GFs/PEDOT-PSS nanocomposite gas sensor upon NH_3 exposure and therefore enhanced NH_3 response.

Conclusion

In this work, novel NH_3 gas sensor based on CuTSPc@3D-(N)GFs/PEDOT-PSS nanocomposite have been successfully fabricated and studied for the first time. The resultant CuTSPc@3D-(N)GFs/PEDOT-PSS nanocomposite exhibited excellent sensivity, dynamic behavior and selectivity to NH_3 owning possibly to the increase of the specific surface area, intrinsic sensing properties of CuTSPc@3D-(N)GF, and π-π interaction in CuTSPc@3D-(N)GFs/PEDOT-PSS. The nanocomposite gas sensor indicated much better (~ 5 and 53 times respectively with the concentration of NH_3 gas at 200 ppm) response to NH_3 gas than those of the sensors based on pure PEDOT-PSS and pristine CuTSPc@3D-(N)GFs. The response and recovery times of nanocomposite gas sensor (2.5 min, and 1 min, respectively) is much lower than that of pure PEDOT-PSS (6 min, and 2.5 min, respectively) towards 200 ppm NH_3. It demonstrates that the CuTSPc@3D-(N)GFs/PEDOT-PSS nanocomposite gas sensor which offers several distinct advantages on NH_3 detection over other fabricated sensors including high sensivity, high productivity, low temperature processing and low cost, is expected to hold great promise for real-world applications.

References

1. Dan, Y., et al., *Intrinsic response of graphene vapor sensors.* Nano Letters, 2009. **9**(4): p. 1472-1475.
2. Lu, G., L.E. Ocola, and J. Chen, *Gas detection using low-temperature reduced graphene oxide sheets.* Applied Physics Letters, 2009. **94**(8): p. 083111.
3. Schedin, F., et al., *Detection of individual gas molecules adsorbed on graphene.* Nature materials, 2007. **6**(9): p. 652-655.
4. Chu, B.H., et al., *Effect of coated platinum thickness on hydrogen detection sensitivity of graphene-based sensors.* Electrochemical and Solid-State Letters, 2011. **14**(7): p. K43-K45.
5. Vedala, H., et al., *Chemical sensitivity of graphene edges decorated with metal nanoparticles.* Nano letters, 2011. **11**(6): p. 2342-2347.
6. Zhang, D., et al., *Room-temperature high-performance acetone gas sensor based on hydrothermal synthesized SnO 2-reduced graphene oxide hybrid composite.* RSC Advances, 2015. **5**(4): p. 3016-3022.
7. Zhang, H., et al., *SnO 2 nanoparticles-reduced graphene oxide nanocomposites for NO 2 sensing at low operating temperature.* Sensors and Actuators B: Chemical, 2014. **190**: p. 472-478.
8. Liu, S., et al., *High performance room temperature NO 2 sensors based on reduced graphene oxide-multiwalled carbon nanotubes-tin oxide nanoparticles hybrids.* Sensors and Actuators B: Chemical, 2015. **211**: p. 318-324.

9. Huang, X., et al., *Reduced graphene oxide–polyaniline hybrid: preparation, characterization and its applications for ammonia gas sensing.* Journal of Materials Chemistry, 2012. **22**(42): p. 22488-22495.
10. Lee, C., et al., *Measurement of the elastic properties and intrinsic strength of monolayer graphene.* science, 2008. **321**(5887): p. 385-388.
11. Stoller, M.D., et al., *Graphene-based ultracapacitors.* Nano letters, 2008. **8**(10): p. 3498-3502.
12. Balandin, A.A., et al., *Superior thermal conductivity of single-layer graphene.* Nano letters, 2008. **8**(3): p. 902-907.
13. Worsley, M.A., et al., *Synthesis of graphene aerogel with high electrical conductivity.* Journal of the American Chemical Society, 2010. **132**(40): p. 14067-14069.
14. Tang, Z., et al., *Noble-metal-promoted three-dimensional macroassembly of single-layered graphene oxide.* Angewandte Chemie, 2010. **122**(27): p. 4707-4711.
15. Lee, S.H., et al., *Three-Dimensional Self-Assembly of Graphene Oxide Platelets into Mechanically Flexible Macroporous Carbon Films.* Angewandte Chemie International Edition, 2010. **49**(52): p. 10084-10088.
16. Chen, Z., et al., *Three-dimensional flexible and conductive interconnected graphene networks grown by chemical vapour deposition.* Nature materials, 2011. **10**(6): p. 424-428.
17. Wu, Z.-S., et al., *Three-dimensional graphene-based macro-and mesoporous frameworks for high-performance electrochemical capacitive energy storage.* Journal of the American Chemical Society, 2012. **134**(48): p. 19532-19535.
18. Wu, Z.S., et al., *Three-Dimensional Nitrogen and Boron Co-doped Graphene for High-Performance All-Solid-State Supercapacitors.* Advanced Materials, 2012. **24**(37): p. 5130-5135.
19. Choi, B.G., et al., *3D macroporous graphene frameworks for supercapacitors with high energy and power densities.* ACS nano, 2012. **6**(5): p. 4020-4028.
20. Cao, X., et al., *Preparation of novel 3D graphene networks for supercapacitor applications.* Small, 2011. **7**(22): p. 3163-3168.
21. Xiao, J., et al., *Hierarchically porous graphene as a lithium–air battery electrode.* Nano letters, 2011. **11**(11): p. 5071-5078.
22. Chen, W., et al., *Self-Assembly and Embedding of Nanoparticles by In Situ Reduced Graphene for Preparation of a 3D Graphene/Nanoparticle Aerogel.* Advanced materials, 2011. **23**(47): p. 5679-5683.
23. Wu, Z.-S., et al., *3D nitrogen-doped graphene aerogel-supported Fe3O4 nanoparticles as efficient electrocatalysts for the oxygen reduction reaction.* Journal of the American Chemical Society, 2012. **134**(22): p. 9082-9085.
24. Yong, Y.-C., et al., *Macroporous and monolithic anode based on polyaniline hybridized three-dimensional graphene for high-performance microbial fuel cells.* ACS nano, 2012. **6**(3): p. 2394-2400.
25. SadegháLaeini, M., *Aqueous aerobic oxidation of alkyl arenes and alcohols catalyzed by copper (II) phthalocyanine supported on three-dimensional nitrogen-doped graphene at room temperature.* Chemical Communications, 2014. **50**(58): p. 7855-7857.
26. Dong, X., et al., *3D graphene foam as a monolithic and macroporous carbon electrode for electrochemical sensing.* ACS applied materials & interfaces, 2012. **4**(6): p. 3129-3133.
27. Seekaew, Y., et al., *Low-cost and flexible printed graphene–PEDOT: PSS gas sensor for ammonia detection.* Organic Electronics, 2014. **15**(11): p. 2971-2981.
28. Timpanaro, S., et al., *Morphology and conductivity of PEDOT/PSS films studied by scanning–tunneling microscopy.* Chemical Physics Letters, 2004. **394**(4): p. 339-343.
29. Nardes, A.M., et al., *Conductivity, work function, and environmental stability of PEDOT: PSS thin films treated with sorbitol.* Organic Electronics, 2008. **9**(5): p. 727-734.

30. Wu, X., et al., *Flexible organic light emitting diodes based on double-layered graphene/PEDOT: PSS conductive film formed by spray-coating.* Vacuum, 2014. **101**: p. 53-56.
31. Jian, J., et al., *Gas-sensing characteristics of dielectrophoretically assembled composite film of oxygen plasma-treated SWCNTs and PEDOT/PSS polymer.* Sensors and Actuators B: Chemical, 2013. **178**: p. 279-288.
32. Dehsari, H.S., et al., *Efficient preparation of ultralarge graphene oxide using a PEDOT: PSS/GO composite layer as hole transport layer in polymer-based optoelectronic devices.* RSC Advances, 2014. **4**(98): p. 55067-55076.
33. Mahyari, M., A. Shaabani, and Y. Bide, *Gold nanoparticles supported on supramolecular ionic liquid grafted graphene: a bifunctional catalyst for the selective aerobic oxidation of alcohols.* RSC Advances, 2013. **3**(44): p. 22509-22517.
34. Mahyari, M. and A. Shaabani, *Nickel nanoparticles immobilized on three-dimensional nitrogen-doped graphene as a superb catalyst for the generation of hydrogen from the hydrolysis of ammonia borane.* Journal of Materials Chemistry A, 2014. **2**(39): p. 16652-16659.
35. Hasani, A., et al., *Sensor for volatile organic compounds using an interdigitated gold electrode modified with a nanocomposite made from poly (3, 4-ethylenedioxythiophene)-poly (styrenesulfonate) and ultra-large graphene oxide.* Microchimica Acta, 2015. **182**(7-8): p. 1551-1559.
36. Gavgani, J.N., et al., *A room temperature volatile organic compound sensor with enhanced performance, fast response and recovery based on N-doped graphene quantum dots and poly (3, 4-ethylenedioxythiophene)–poly (styrenesulfonate) nanocomposite.* RSC Advances, 2015. **5**(71): p. 57559-57567.
37. Hosseini, H., et al., *Ordered carbohydrate-derived porous carbons immobilized gold nanoparticles as a new electrode material for electrocatalytical oxidation and determination of nicotinamide adenine dinucleotide.* Biosensors and Bioelectronics, 2014. **59**: p. 412-417.
38. McAllister, M.J., et al., *Single sheet functionalized graphene by oxidation and thermal expansion of graphite.* Chemistry of Materials, 2007. **19**(18): p. 4396-4404.
39. Lin, C.-Y., et al., *Using a PEDOT: PSS modified electrode for detecting nitric oxide gas.* Sensors and Actuators B: Chemical, 2009. **140**(2): p. 402-406.
40. Xu, J., et al., *Self-assembly of conducting polymer nanowires at air–water interface and its application for gas sensors.* Materials Science and Engineering: B, 2009. **157**(1): p. 87-92.
41. Kwon, O.S., et al., *Novel flexible chemical gas sensor based on poly (3, 4-ethylenedioxythiophene) nanotube membrane.* Talanta, 2010. **82**(4): p. 1338-1343.
42. Yoo, K.-P., et al., *Effects of O 2 plasma treatment on NH 3 sensing characteristics of multiwall carbon nanotube/polyaniline composite films.* Sensors and Actuators B: Chemical, 2009. **143**(1): p. 333-340.
43. Tai, H., et al., *Fabrication and gas sensitivity of polyaniline–titanium dioxide nanocomposite thin film.* Sensors and Actuators B: Chemical, 2007. **125**(2): p. 644-650.
44. Matsuguchi, M., et al., *Effect of NH 3 gas on the electrical conductivity of polyaniline blend films.* Synthetic metals, 2002. **128**(1): p. 15-19.
45. Kebiche, H., et al., *Relationship between ammonia sensing properties of polyaniline nanostructures and their deposition and synthesis methods.* Analytica chimica acta, 2012. **737**: p. 64-71.
46. Hong, L., Y. Li, and M. Yang, *Fabrication and ammonia gas sensing of palladium/polypyrrole nanocomposite.* Sensors and Actuators B: Chemical, 2010. **145**(1): p. 25-31.
47. Crowley, K., et al., *Fabrication of an ammonia gas sensor using inkjet-printed polyaniline nanoparticles.* Talanta, 2008. **77**(2): p. 710-717.

48. Verma, D. and V. Dutta, *Role of novel microstructure of polyaniline-CSA thin film in ammonia sensing at room temperature.* Sensors and Actuators B: Chemical, 2008. **134**(2): p. 373-376.
49. Sengupta, P.P., P. Kar, and B. Adhikari, *Influence of dopant in the synthesis, characteristics and ammonia sensing behavior of processable polyaniline.* Thin Solid Films, 2009. **517**(13): p. 3770-3775.
50. Suchea, M., et al., *Low temperature indium oxide gas sensors.* Sensors and Actuators B: Chemical, 2006. **118**(1): p. 135-141.
51. Bekyarova, E., et al., *Chemically functionalized single-walled carbon nanotubes as ammonia sensors.* The Journal of Physical Chemistry B, 2004. **108**(51): p. 19717-19720.
52. Huang, J., et al., *Polyaniline nanofibers: facile synthesis and chemical sensors.* Journal of the American Chemical Society, 2003. **125**(2): p. 314-315.
53. Virji, S., et al., *Polyaniline nanofiber gas sensors: examination of response mechanisms.* Nano letters, 2004. **4**(3): p. 491-496.
54. Wu, Z., et al., *Enhanced sensitivity of ammonia sensor using graphene/polyaniline nanocomposite.* Sensors and Actuators B: Chemical, 2013. **178**: p. 485-493.
55. Matsuguchi, M., A. Okamoto, and Y. Sakai, *Effect of humidity on NH 3 gas sensitivity of polyaniline blend films.* Sensors and Actuators B: Chemical, 2003. **94**(1): p. 46-52.

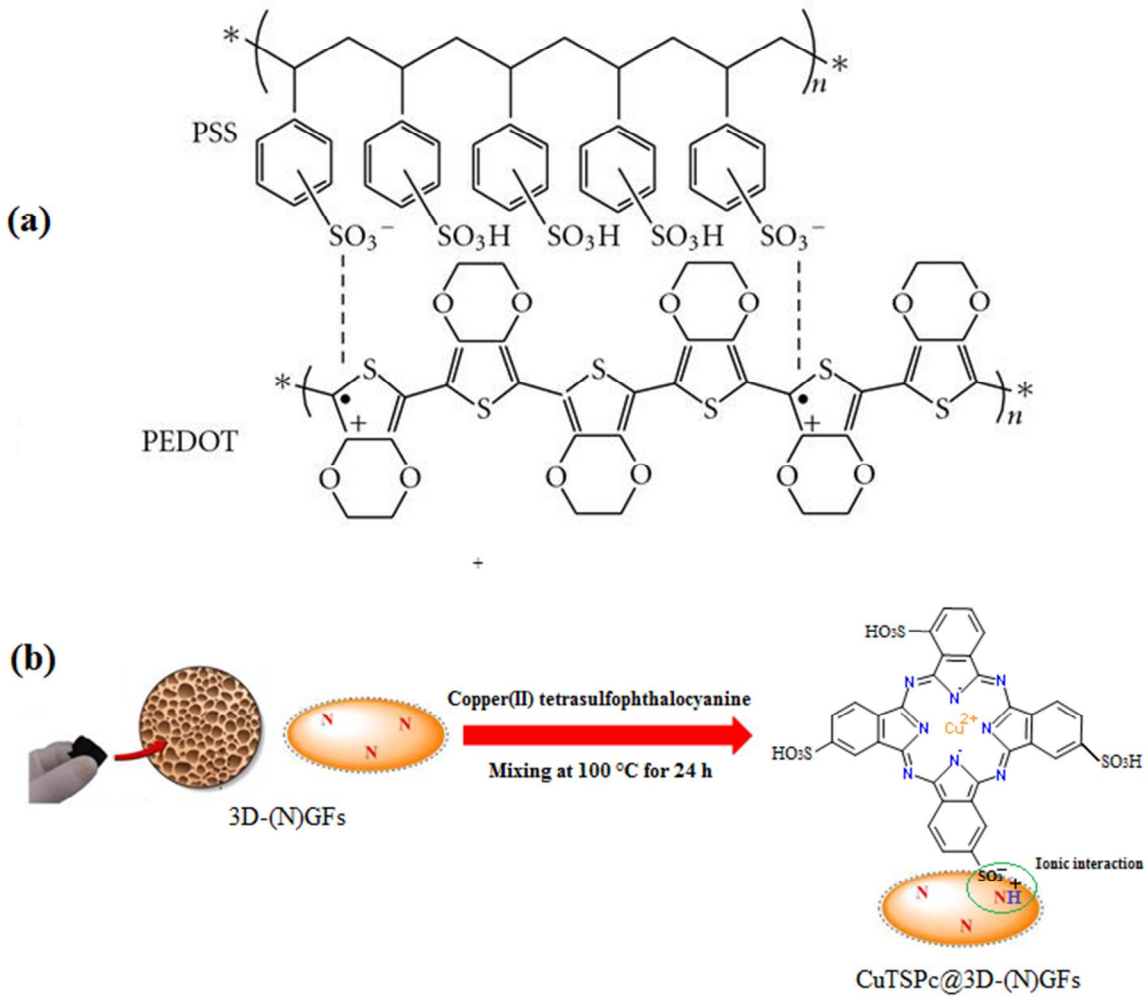

Fig. 1 Schematic structures of (a) PEDOT-PSS, and (b) CuTSPc@3D-(N)GFs.

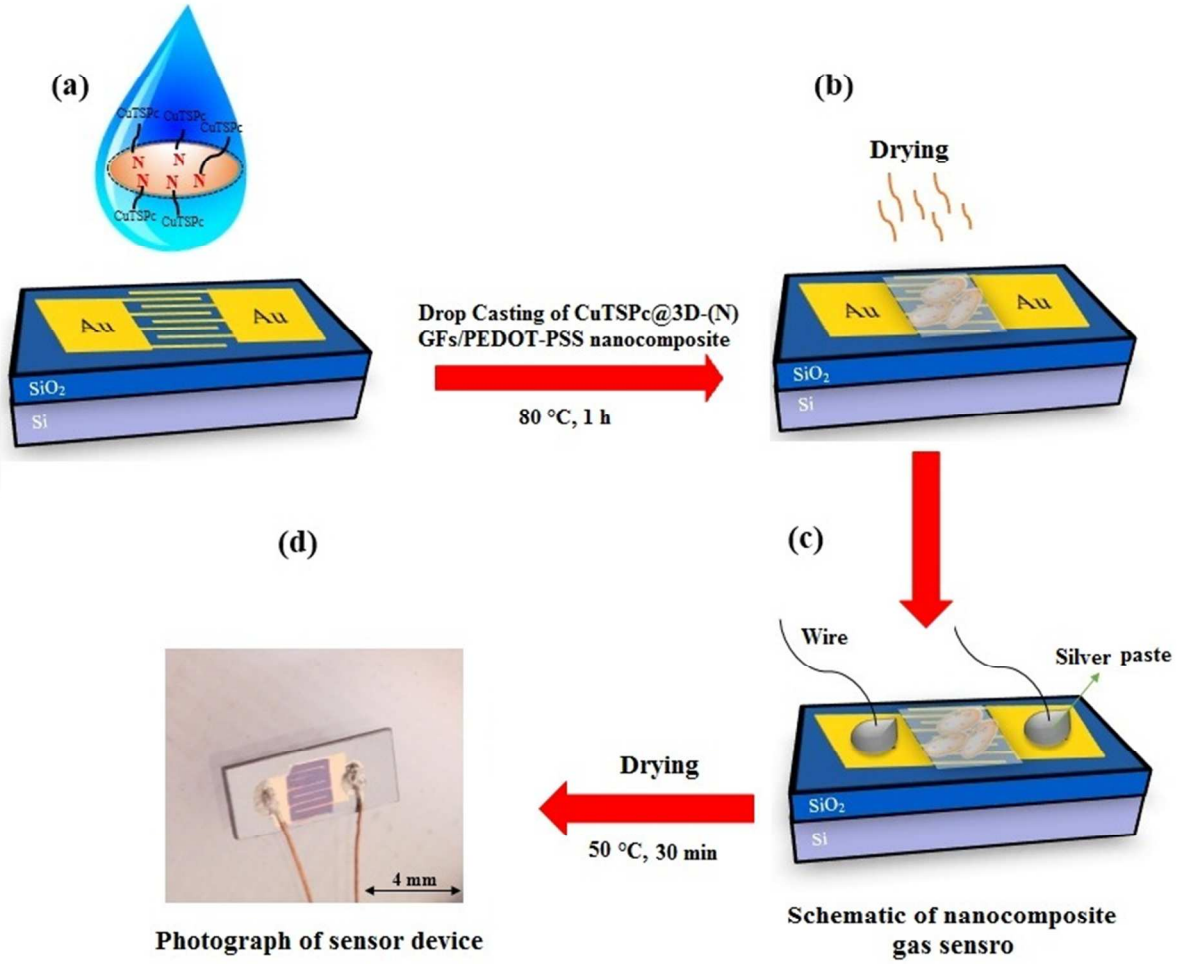

Fig. 2 Schematic steps of gas sensor fabrication process.

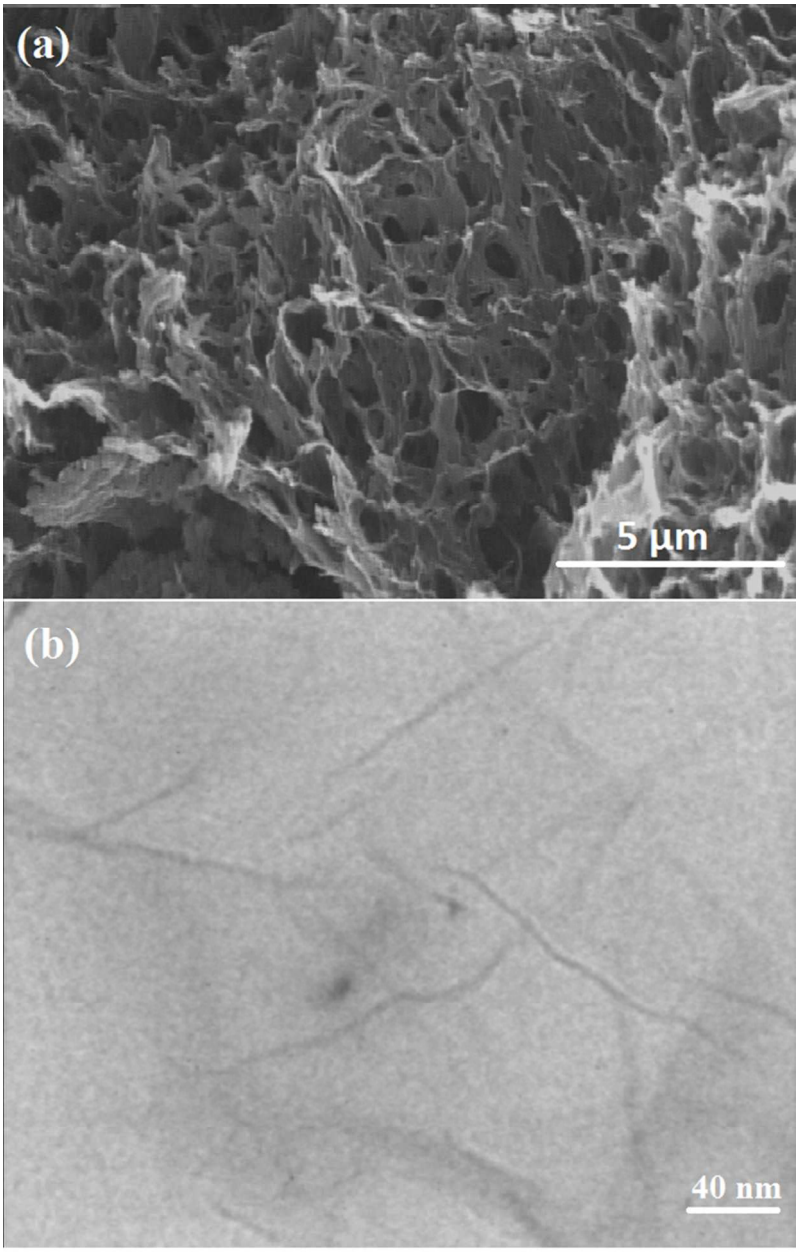

Fig. 3 Microstructure of as-prepared CuTSPc@3D-(N)GFs: (a) SEM, and (b) TEM images.

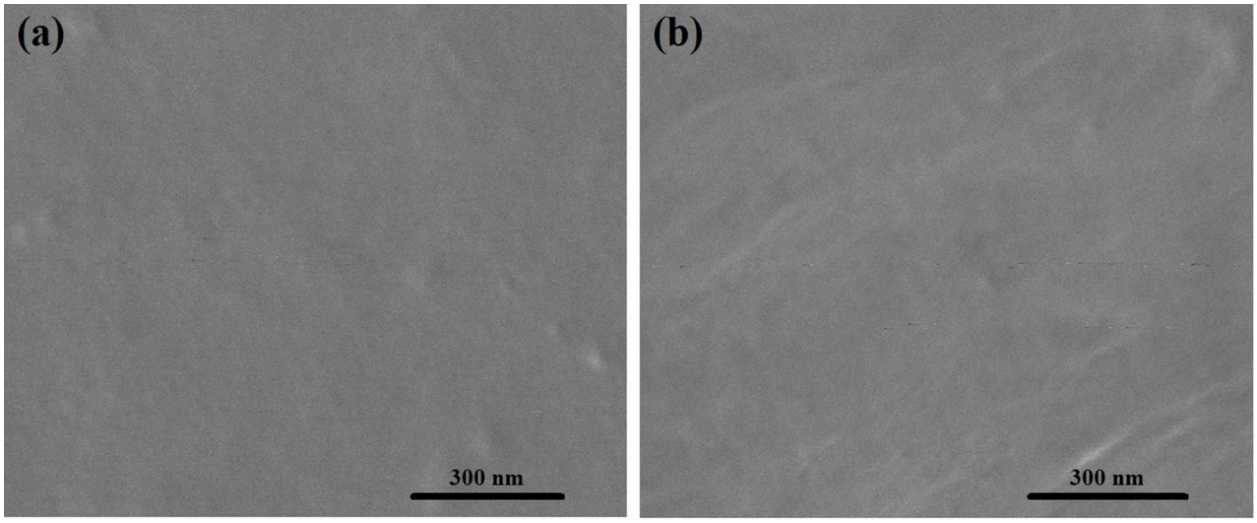

Fig. 4 SEM images of the pure PEDOT-PSS (a), and CuTSPc@3D-(N)GFs/PEDOT-PSS nanocomposite films (b).

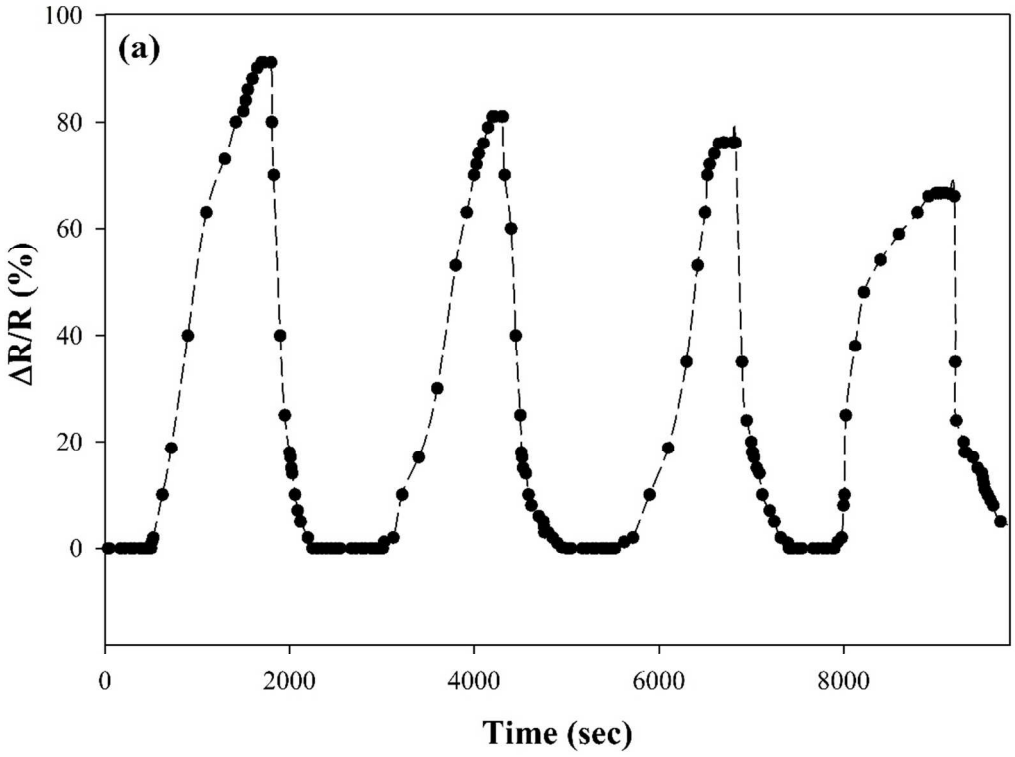

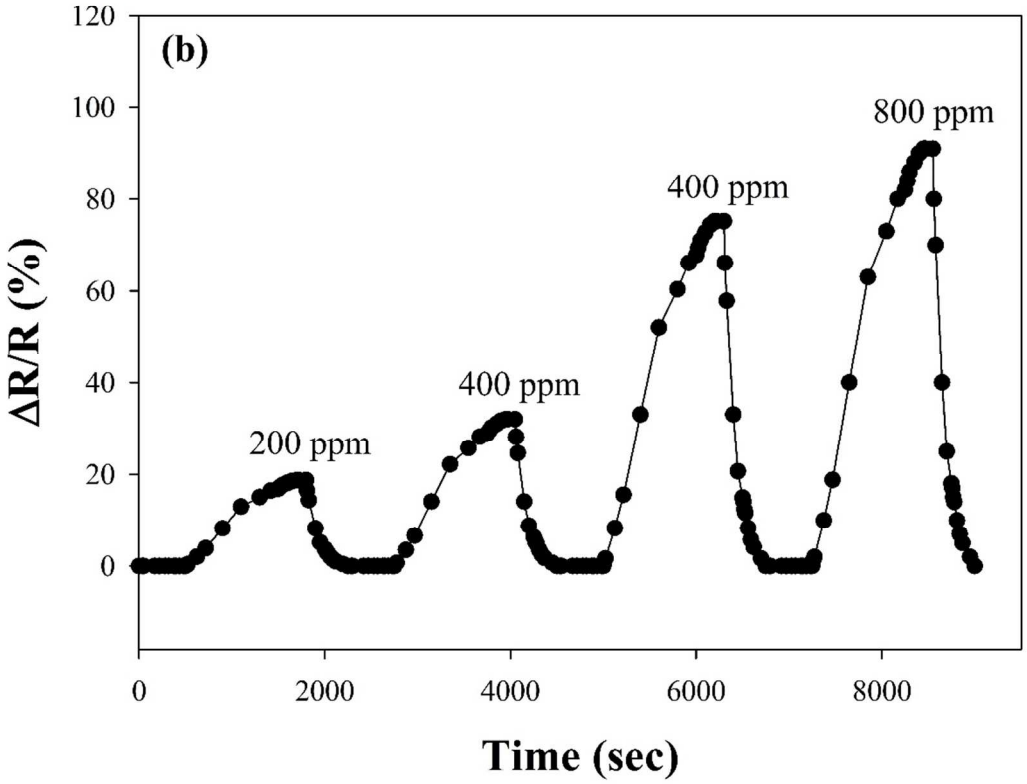

Fig. 5 (a) Dynamic responses of the CuTSPc@3D-(N)GFs/PEDOT-PSS nanocomposite gas sensor to 1000 ppm NH_3, and (b) Sensivity of the CuTSPc@3D-(N)GFs/PEDOT-PSS nanocomposite gas sensor exposed to different concentrations of NH_3 at room temperature.

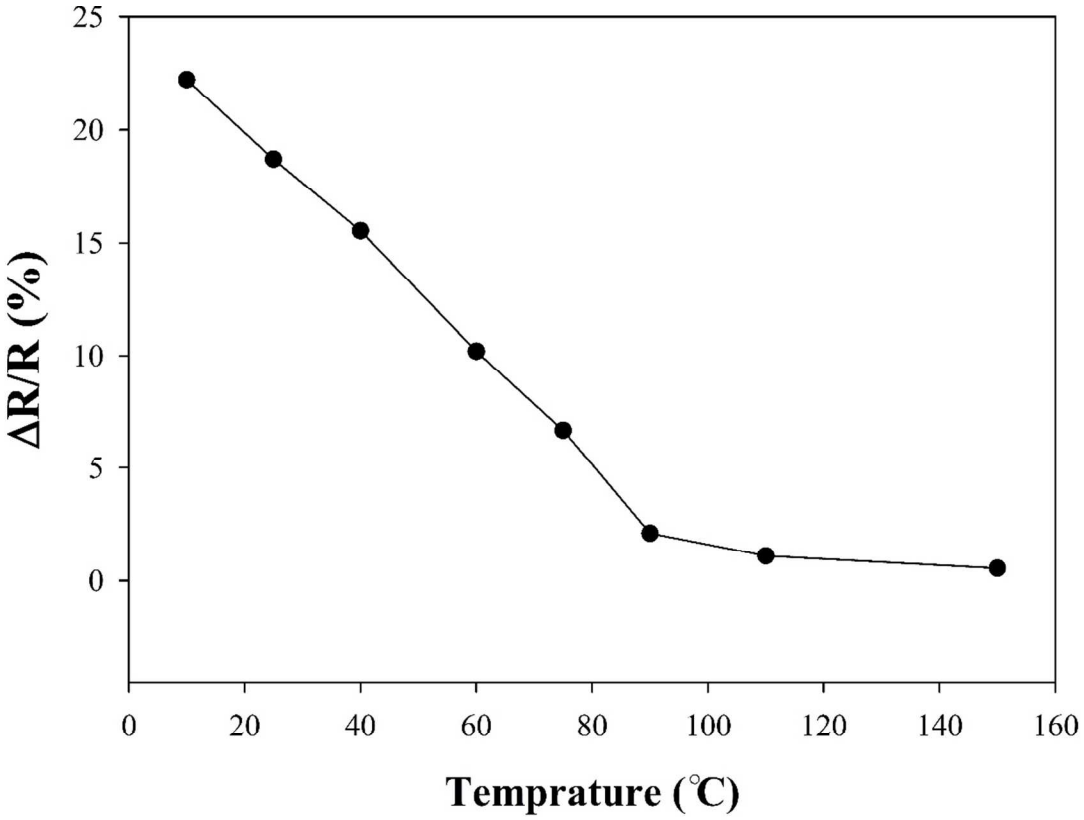

Fig. 6 Sensivity of the CuTSPc@3D-(N)GFs/PEDOT-PSS nanocomposite gas sensor as function of temperature towards 200 ppm NH_3.

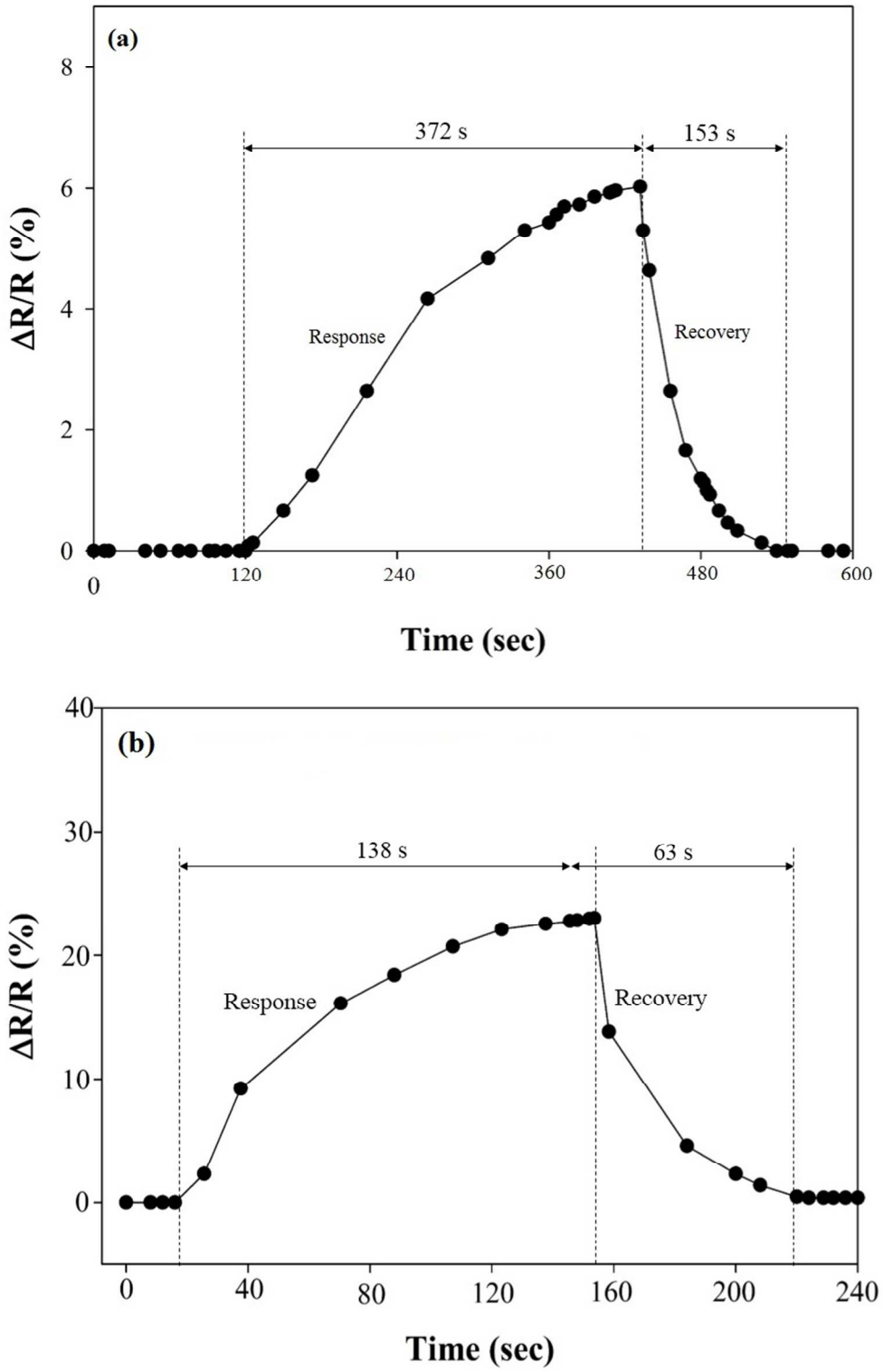

Fig. 7 Response and recovery of gas sensors based on (a) pure PEDOT-PSS, and (b) CuTSPc@3D-(N)GFs/PEDOT-PSS nanocomposite for 200 ppm NH_3 at room temperature.

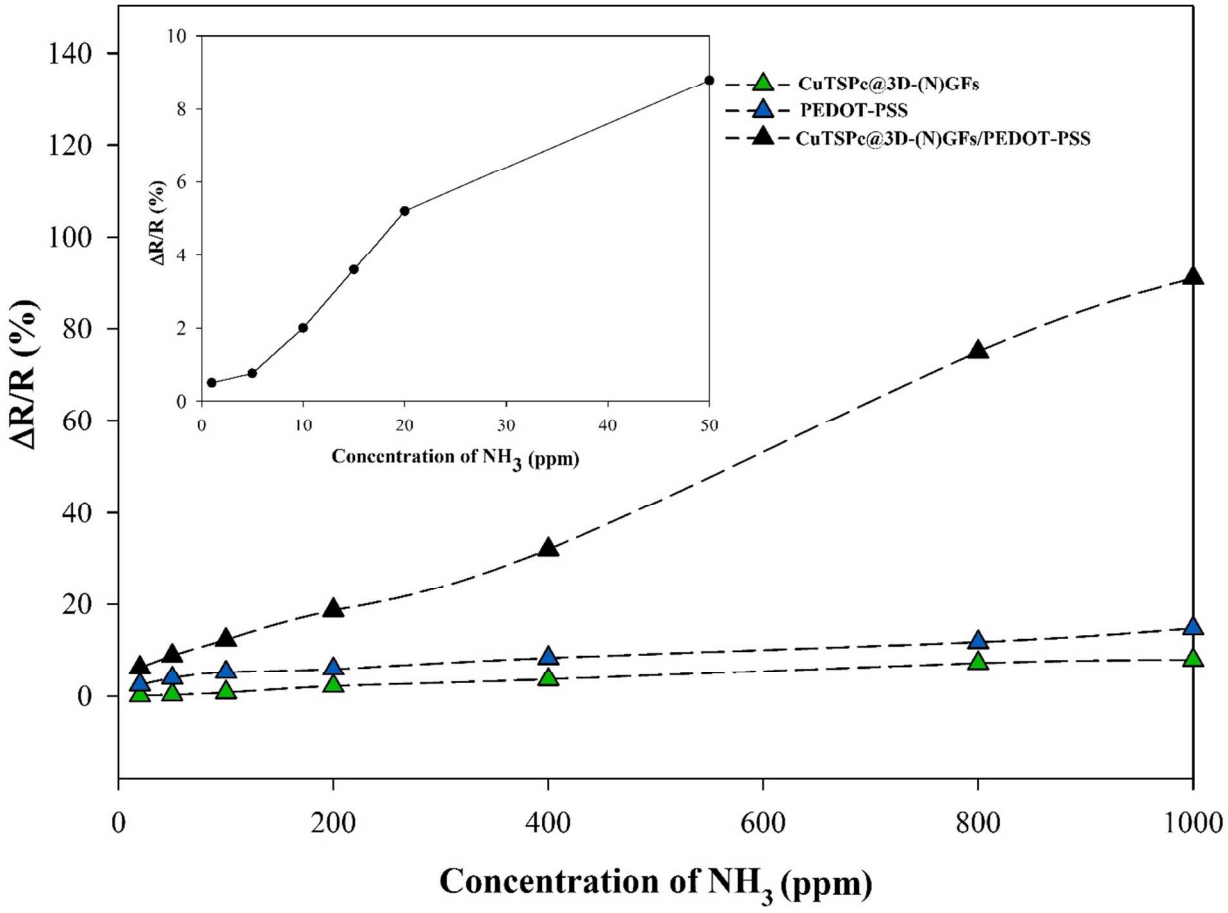

Fig. 8 Sensivity of pure PEDOT-PSS, pristine CuTSPc@3D-(N)GFs and CuTSPc@3D-(N)GFs/PEDOT-PSS nanocomposite gas sensors towards 1-1000 ppm of NH_3 at room temperature.

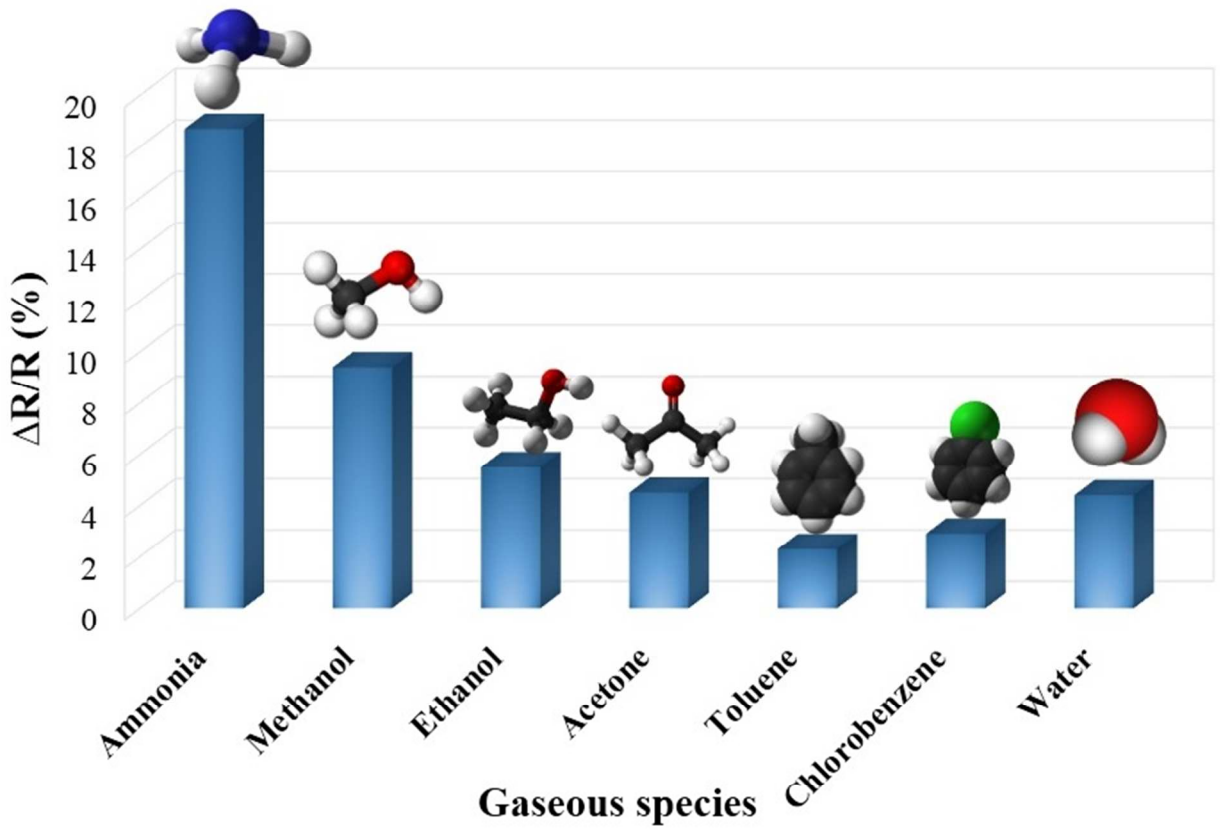

Fig. 9 Selectivity of the CuTSPc@3D-(N)GFs/PEDOT-PSS nanocomposite gas sensor to various VOCs vapors of 200 ppm.

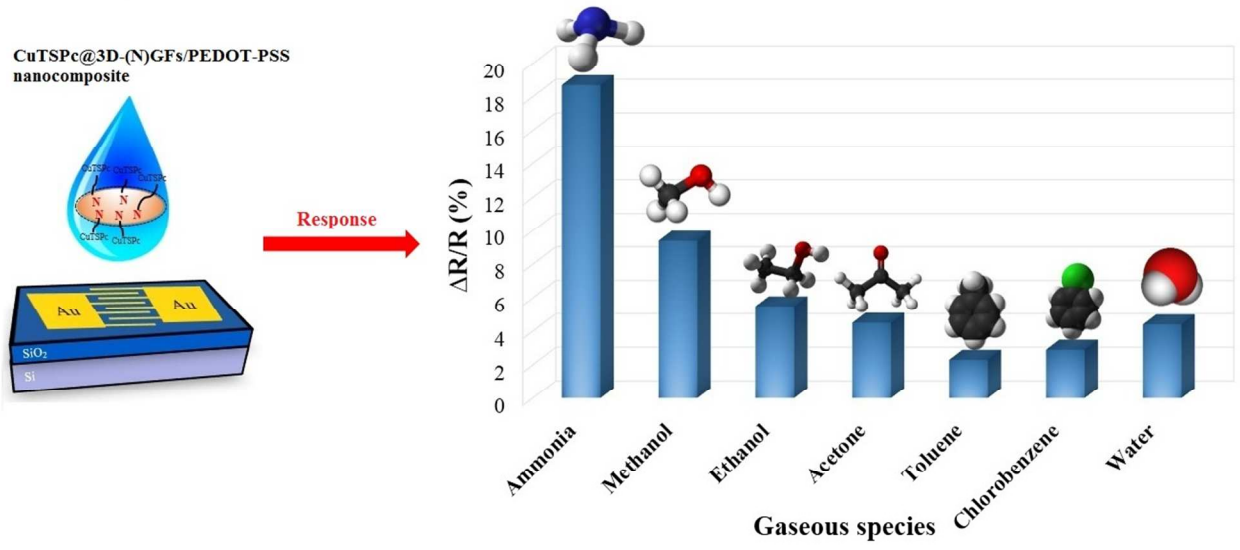

The novel CuTSPc@3D-(N)GFs)/PEDOT-PSS nanocomposite gas sensor allowed excellent sensitivity and selectivity to NH_3 at room temperature.